Electronic Supplementary Material (ESI) for Dalton Transactions.

Design of an antenna effective Eu(III)-based metal-organic framework for highly selective sensing of Fe^{3+}

Jia-Qi Wu, Xin-Yue Ma, Jian-Mei Lu*, Qian Shi* and Li-Xiong Shao*

College of Chemistry and Materials Engineering, Wenzhou University, Chashan University Town, Wenzhou, Zhejiang Province 325035, People's Republic of China.

Table S1. Crystal data and structure refinements for SLX-1

compound	SLX-1
formula	$C_{37}H_{30}EuNO_{11}$
formula weight	816.58
temperature (K)	212.97 K
crystal system	Triclinic
space group	P-1
a (Å)	10.6648(4)
b (Å)	10.9074(4)
c (Å)	17.4597(7)
α (deg)	97.4790(10)
β (deg)	101.0320(10)
γ (deg)	97.9230(10)
V (Å3)	1948.68(13)
Z	2
Dc (g cm^{-3})	1.392
μ (mm^{-1})	1.665
F(000)	820
2θ range (deg)	2.408 to 25.500
GOF on F^2	1.090
reflections collected/unique	28583/7245
R_{int}	0.0593
R_1,[a] wR_2[b] [$I > 2\sigma(I)$]	$R_1 = 0.0440$, $wR^2 = 0.1094$
R_1, wR_2 (all data)	$R_1 = 0.0540$, $wR^2 = 0.1161$
residues (e·$Å^{-3}$)	1.545 / -1.113

[a] $R_1 = \sum (|F_0| - |F_c|) / \sum |F_0|$. [b] $wR_2 = [\sum \{w (|F_0|^2 - |F_c|^2)^2\} / \sum [w (|F_0|^2)^2]]^{1/2}$.

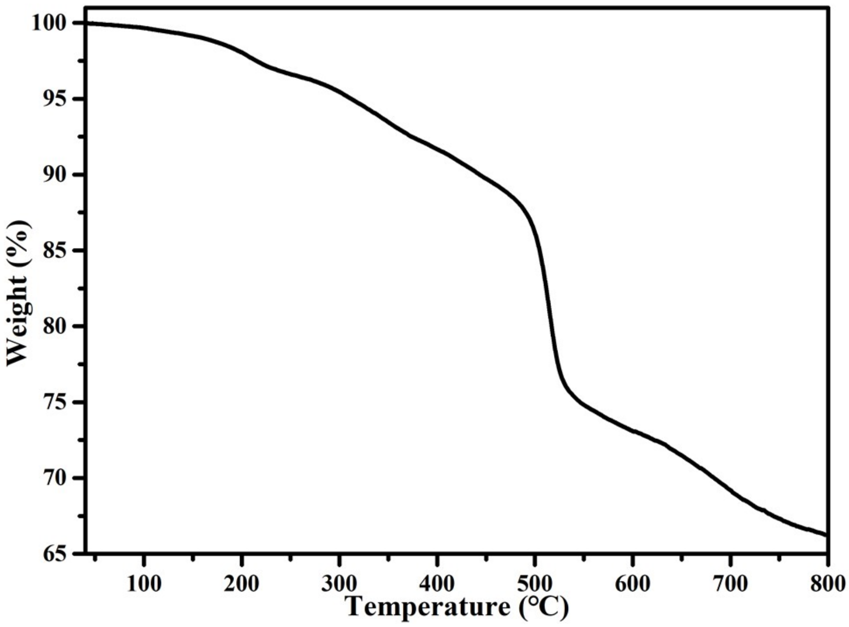

Fig. S1. TGA curve of SLX-1.

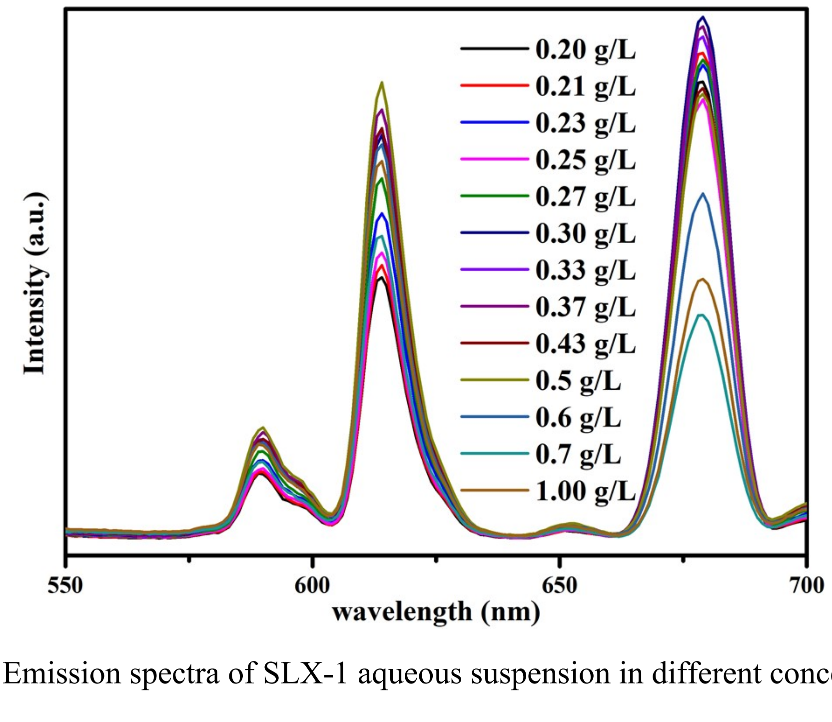

Fig. S2. Emission spectra of SLX-1 aqueous suspension in different concentration.

Table S2. Quenching percentage (QP) of various cations.

Entry	Cations	QP/%
1	Na^{+}	-0.7
2	Blank	0.0
3	Ni^{2+}	0.6
4	Mg^{2+}	0.6
5	Zn^{2+}	1.4
6	Fe^{2+}	1.7
7	Cu^{2+}	2.8
8	Cd^{2+}	3.7
9	NH_4^{+}	3.8
10	K^{+}	4.8
11	Zr^{4+}	8.8
12	Co^{2+}	8.8
13	Fe^{3+}	95.3

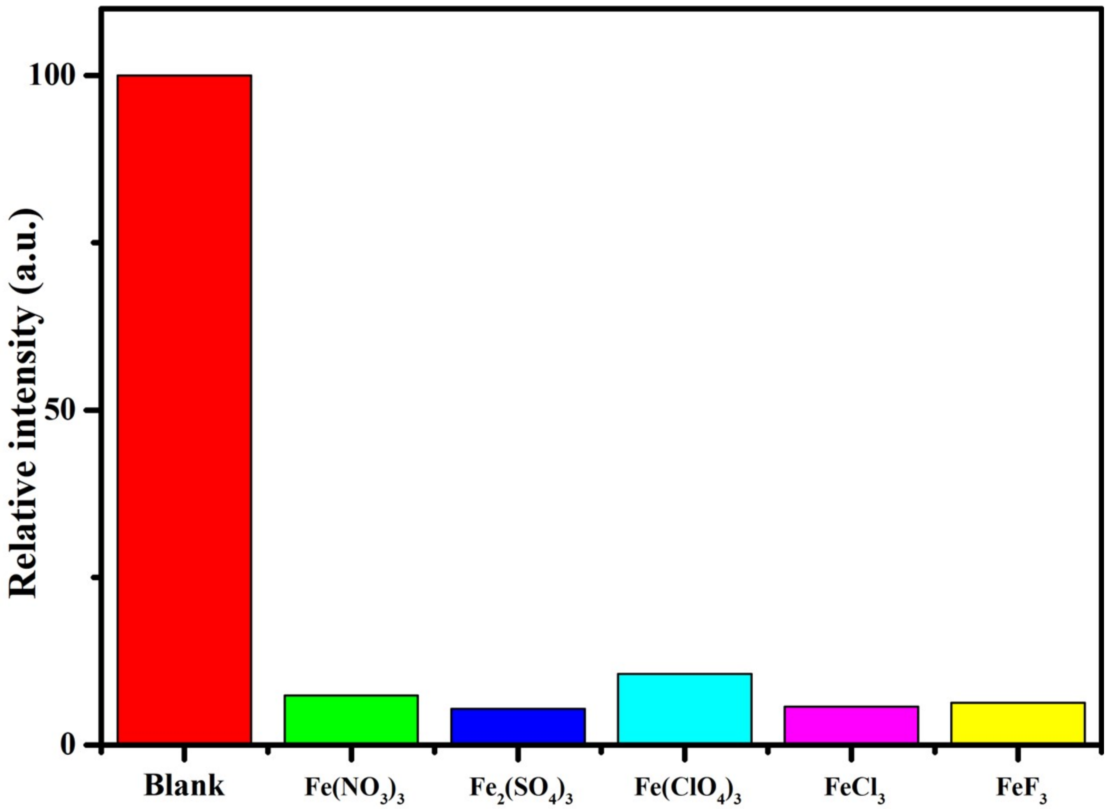

Fig. S3 Emission intensity of SLX-1 at 614 nm after dispersion in various Fe(III) salts.

Table S3. Quenching percentage (QP) of various Fe(III) salts.

Entry	Fe(III) salts	QP/%
1	Blank	0.0
2	$Fe(NO_3)_3$	93.9
3	$Fe_2(SO_4)_3$	95.5
4	$Fe(ClO_4)_3$	91.3
5	FeF_3	94.8
6	$FeCl_3$	95.3

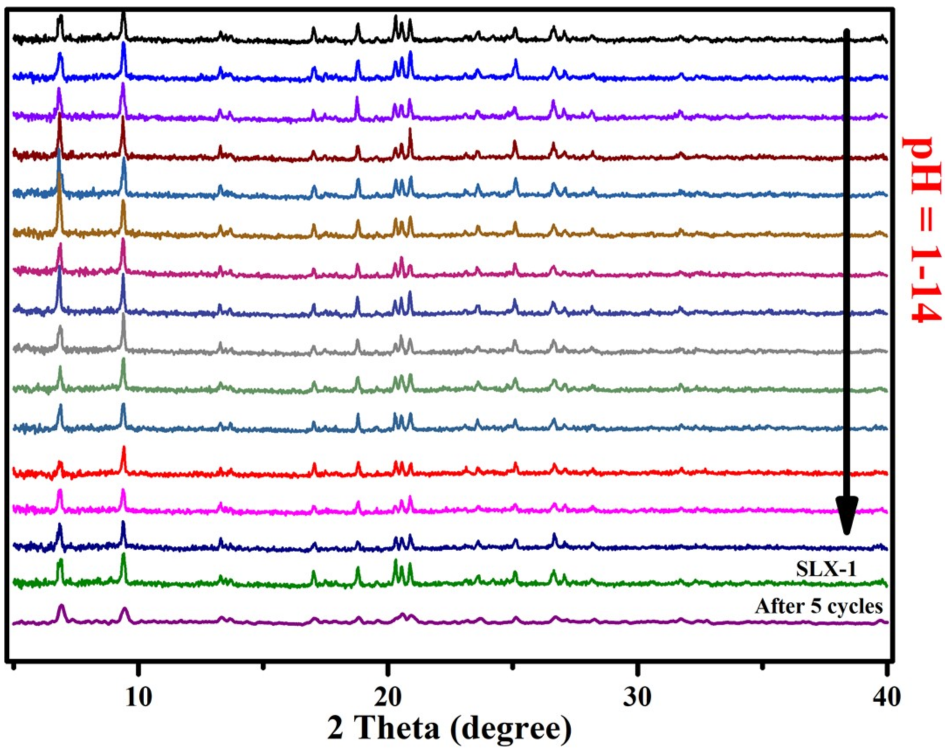

Fig. S4. PXRD spectra of SLX-1 soaked into different pH solutions and used after 5 cycles (room temperature, 2theta: 5-40 degree).

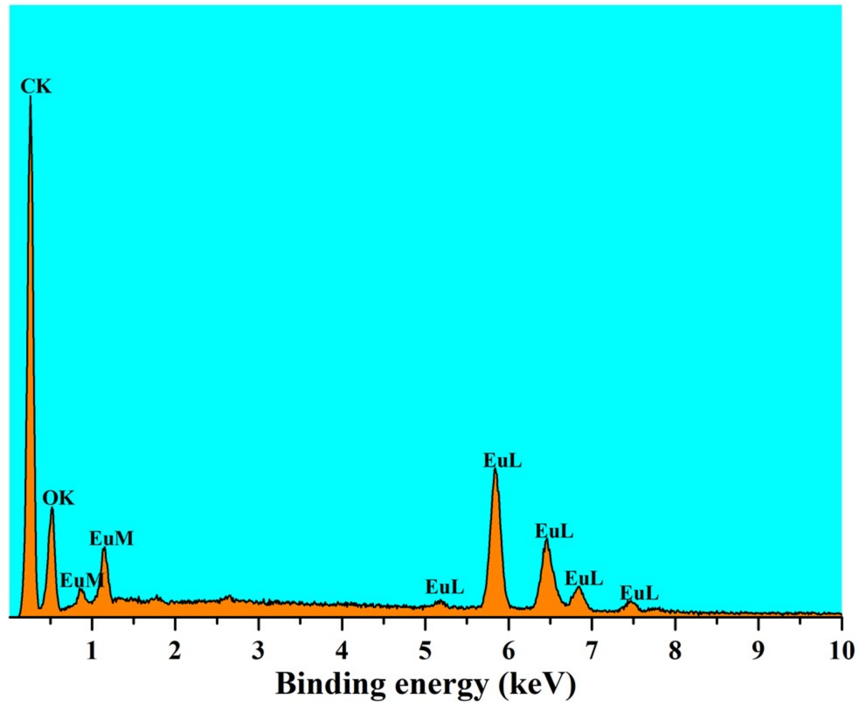

Fig. S5. SEM-EDS of recovered SLX-1 after the sensing of Fe^{3+}.

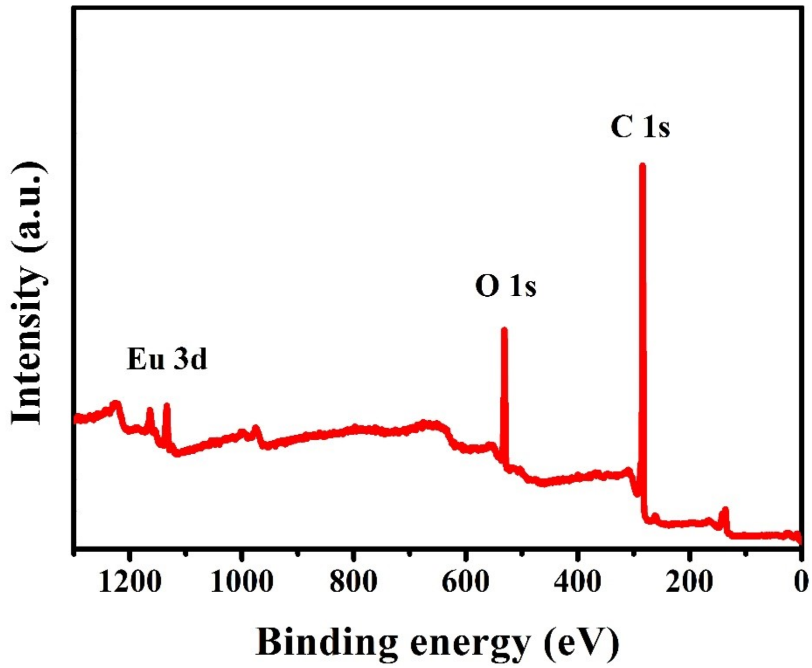

Fig. S6. XPS of recovered SLX-1 after the sensing of Fe^{3+}.

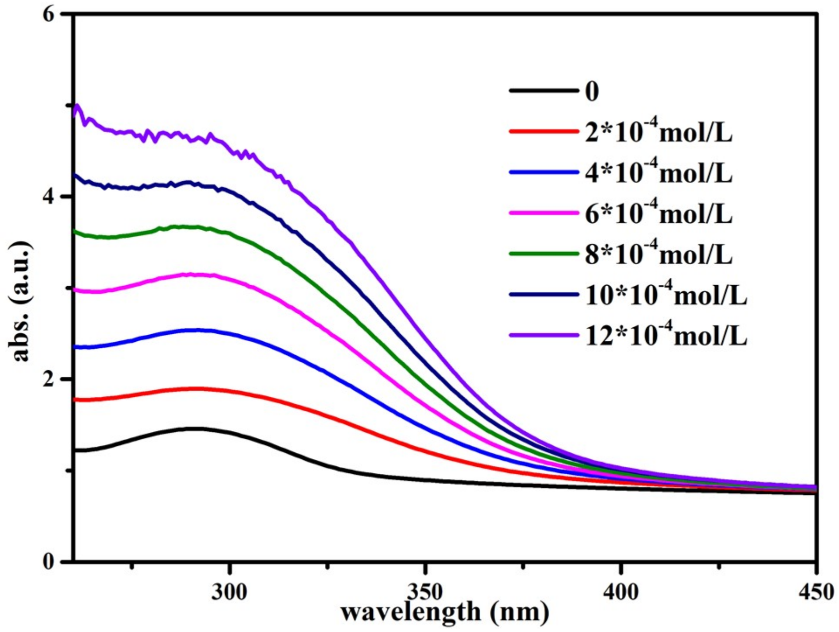

Fig. S7. UV absorption spectrum of SLX-1 suspension titrated by Fe^{3+} ion.

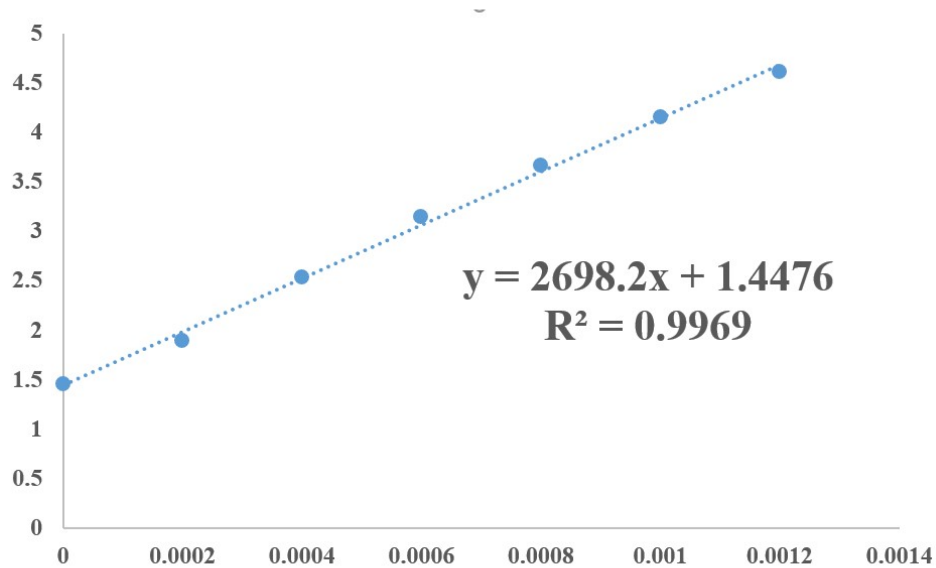

Fig. S8. Linear fitting of the UV absorption intensity of aqueous SLX-1 suspension in the Fe^{3+} titration at wavelength of 290 nm.

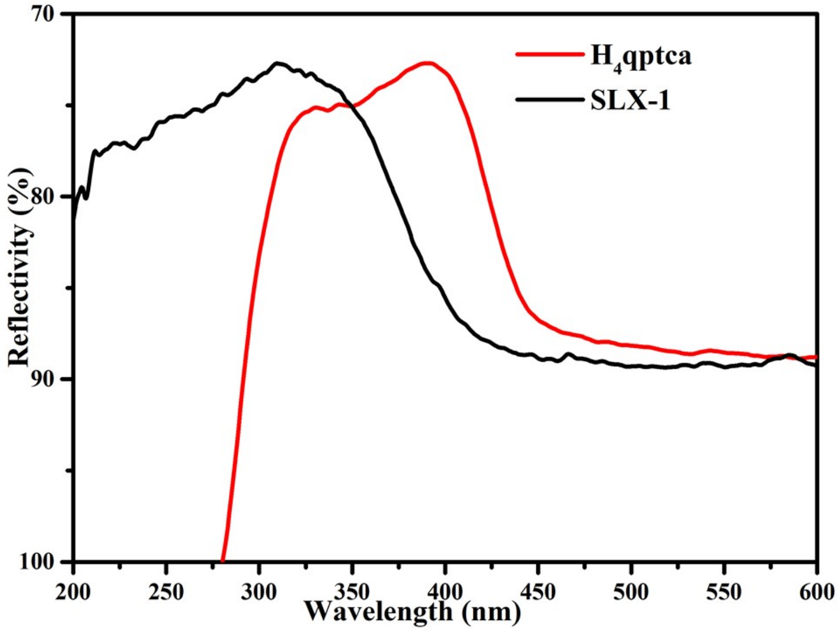

Fig. S9. Solid UV spectrum.

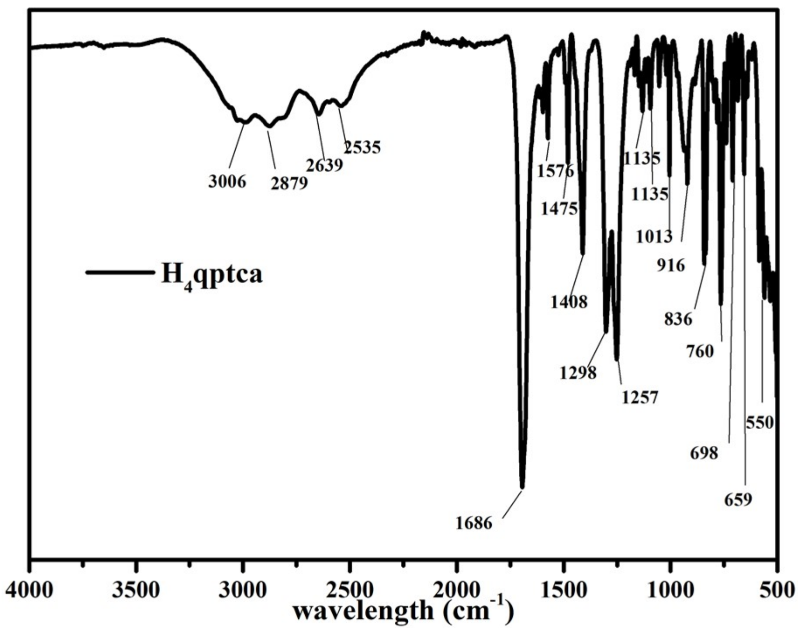

Fig. S10. IR spectrum of H_4qptca.

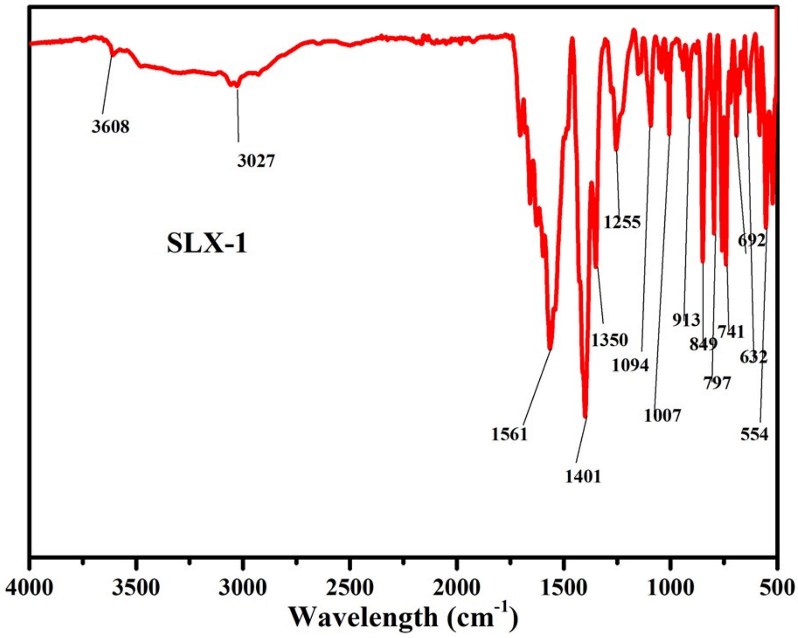

Fig. S11. IR spectrum of SLX-1.

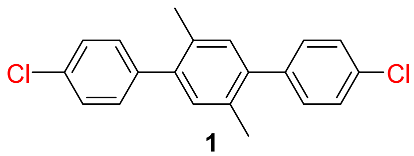
Cl
Cl

1

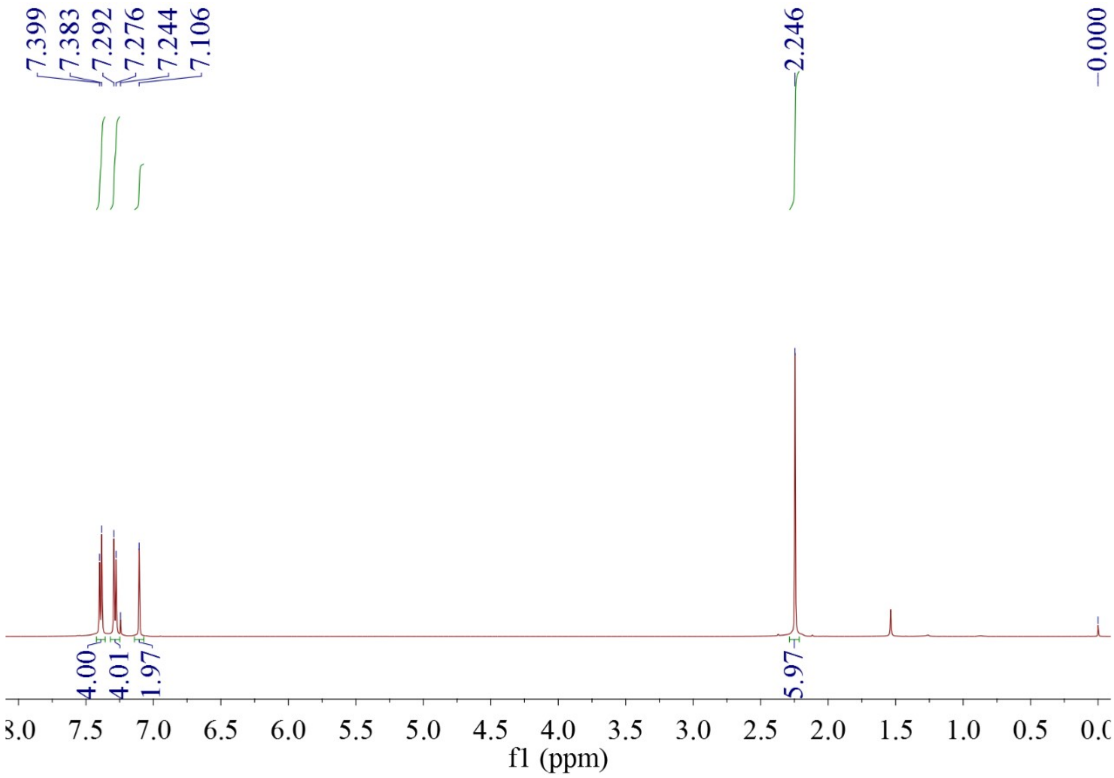
7.399
7.383
7.292
7.276
7.244
7.106
2.246
-0.000
4.00
4.01
1.97
5.97
8.0 7.5 7.0 6.5 6.0 5.5 5.0 4.5 4.0 3.5 3.0 2.5 2.0 1.5 1.0 0.5 0.0
f1 (ppm)

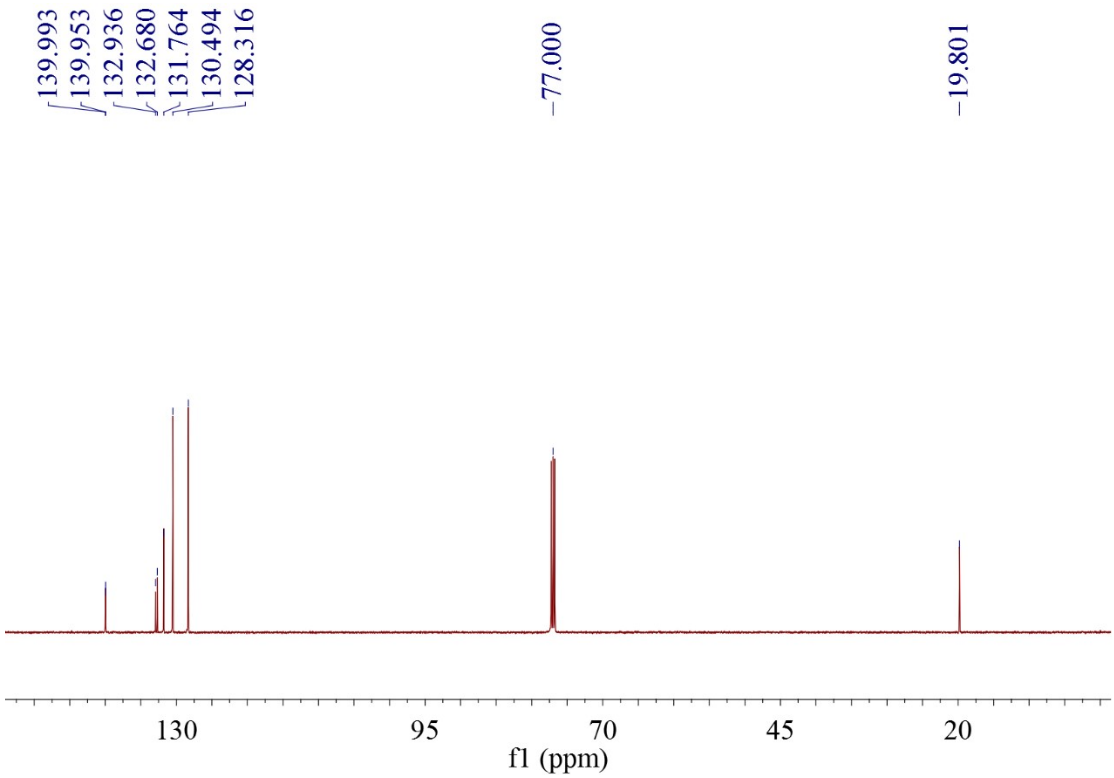
139.993
139.953
132.936
132.680
131.764
130.494
128.316
-77.000
-19.801
130 95 70 45 20
f1 (ppm)

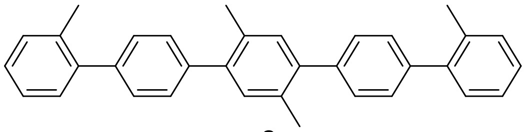

2

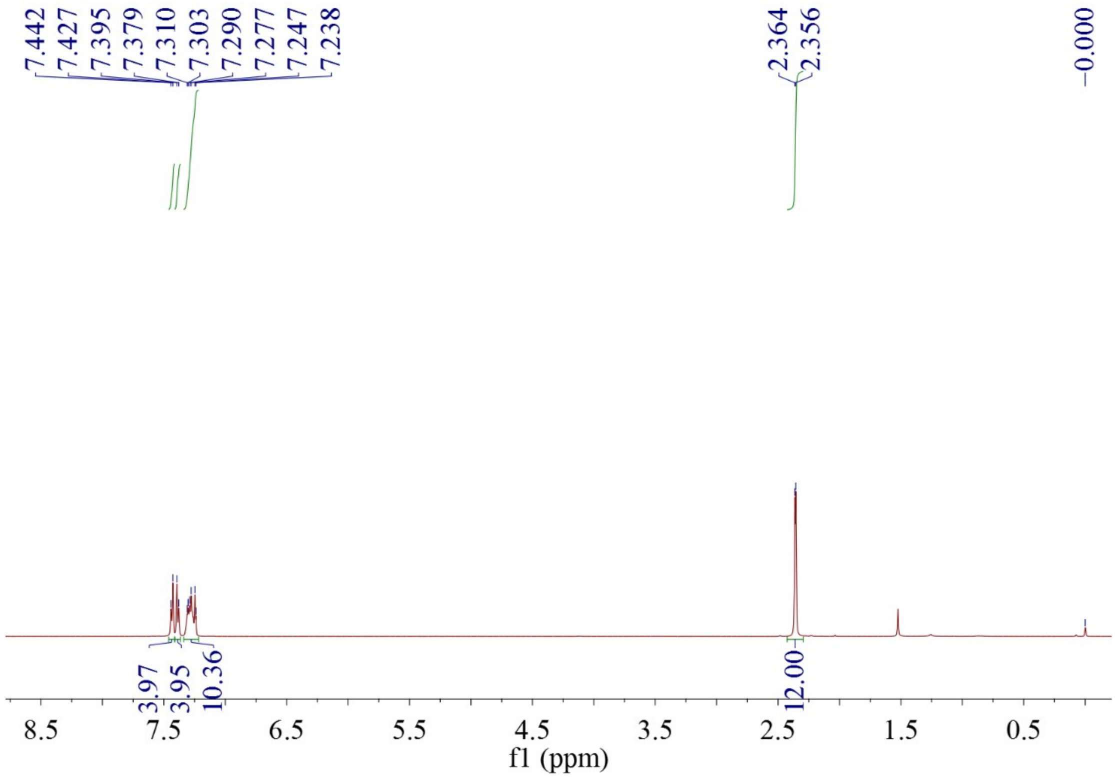
7.442
7.427
7.395
7.379
7.310
7.303
7.290
7.277
7.247
7.238
2.364
2.356
-0.000
3.97
3.95
10.36
12.00
8.5
7.5
6.5
5.5
4.5
3.5
2.5
1.5
0.5
f1 (ppm)

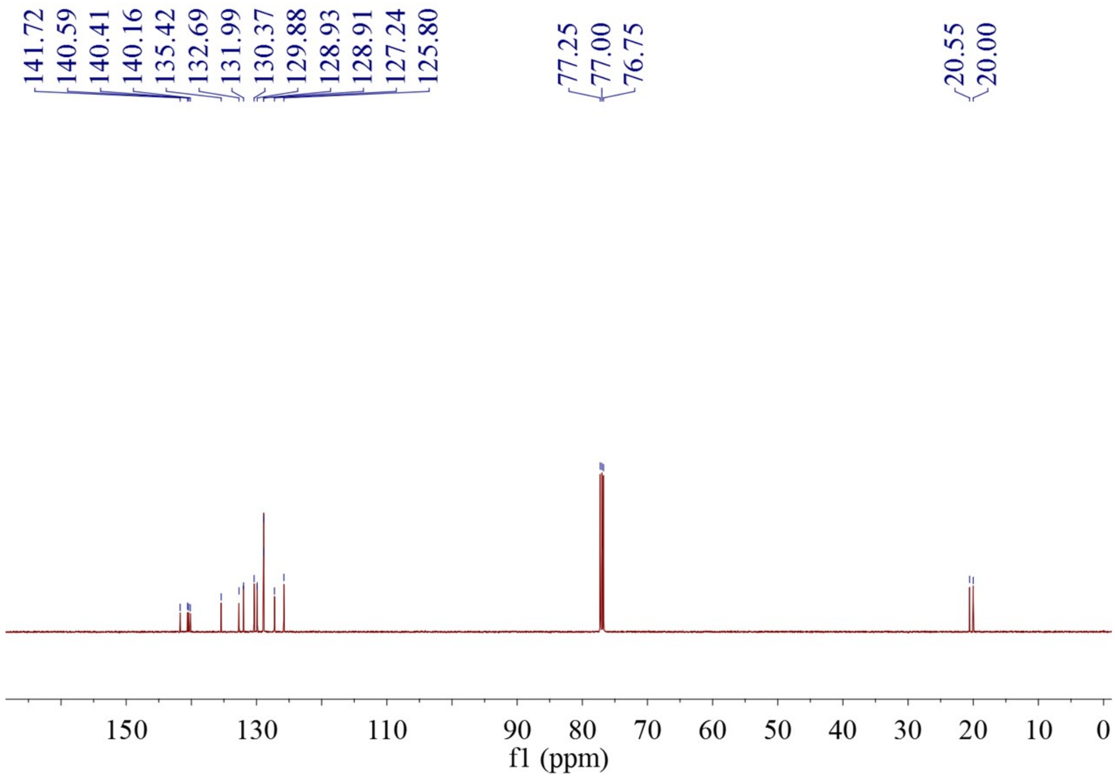
141.72
140.59
140.41
140.16
135.42
132.69
131.99
130.37
129.88
128.93
128.91
127.24
125.80
77.25
77.00
76.75
20.55
20.00
150
130
110
90
80
70
60
50
40
30
20
10
0
f1 (ppm)

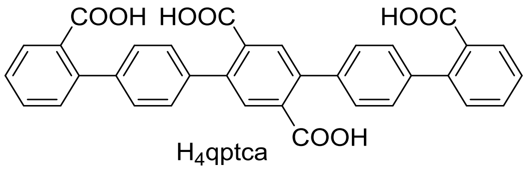
COOH
HOOC
HOOC
COOH

H_4qptca

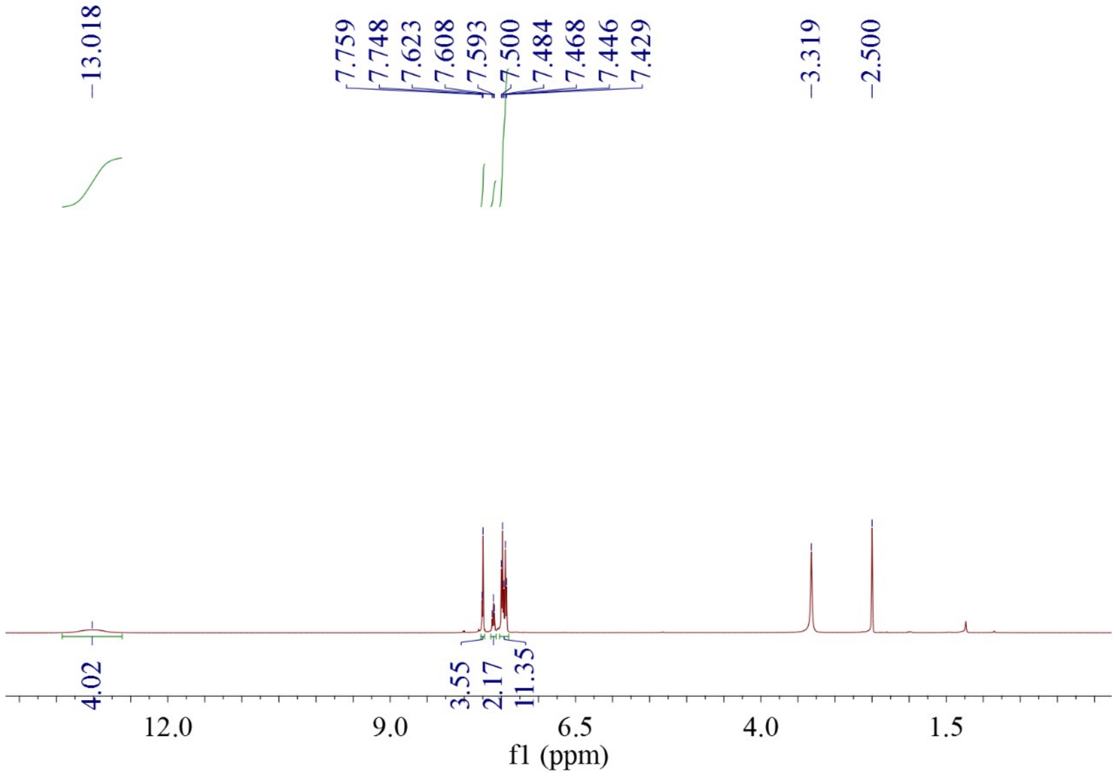
13.018
7.759
7.748
7.623
7.608
7.593
7.500
7.484
7.468
7.446
7.429
3.319
2.500
4.02
3.55
2.17
11.35
12.0
9.0
6.5
4.0
1.5
f1 (ppm)

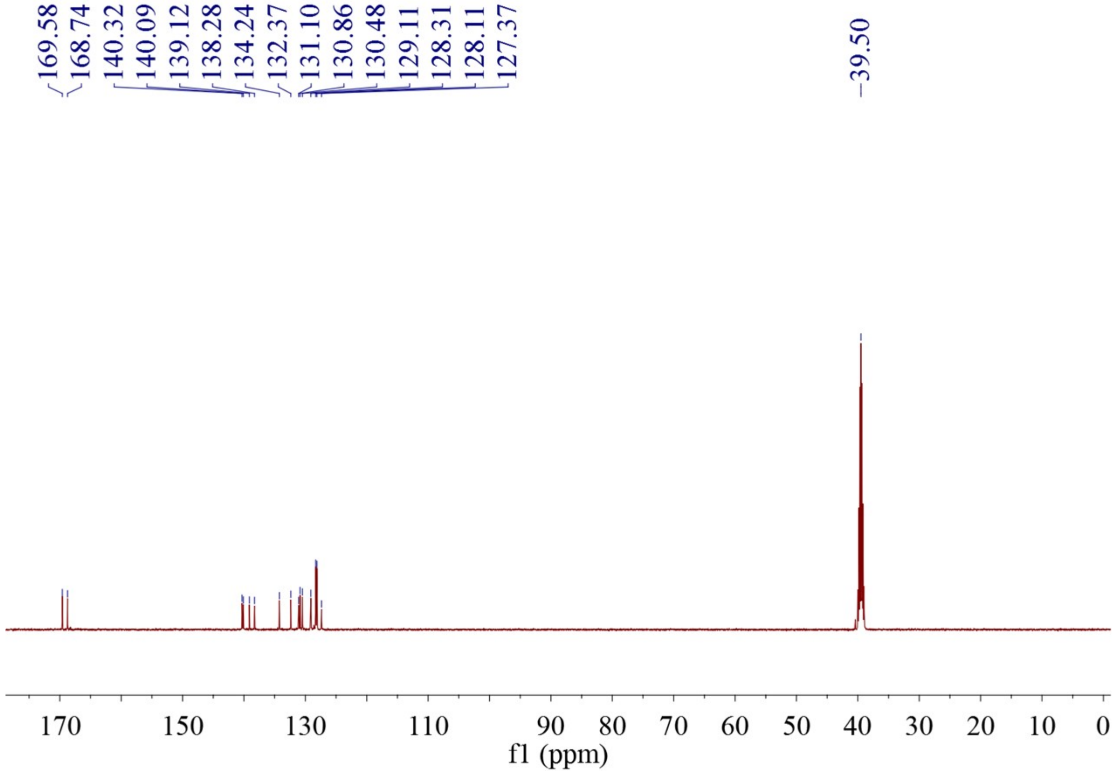
169.58
168.74
140.32
140.09
139.12
138.28
134.24
132.37
131.10
130.86
130.48
129.11
128.31
128.11
127.37
39.50
170
150
130
110
90
80
70
60
50
40
30
20
10
0
f1 (ppm)